Journal of Thermal Analysis and Calorimetry (2021) 143:1221–1229
https://doi.org/10.1007/s10973-020-09578-y

Significance of Joule heating and viscous heating on heat transport of MoS_2–Ag hybrid nanofluid past an isothermal wedge

B. Mahanthesh[1] · S. A. Shehzad[2] · T. Ambreen[3] · S. U. Khan[2]

Received: 16 December 2019 / Accepted: 14 March 2020 / Published online: 23 March 2020

Abstract
The problem of flow and heat transport of magneto-composite nanofluid over an isothermal wedge has not been addressed in the literature up to yet. Thus, this article features the laminar transport of Newtonian composite nanomaterial ($C_2H_6O_2$–H_2O hybrid base liquid + MoS_2–Ag hybrid nanoparticles) in the presence of exponential space- and temperature-dependent heat source past an isothermal wedge. An incompressible and electrically conducting fluid is assumed. The effects of Joule heating and viscous heating are also accounted. Single-phase nanofluid model and boundary layer approximation are utilized to govern the equations of flow and heat transport phenomena. The solution of the simplified coupled system of dimensionless constraints is obtained by using the Runge–Kutta–Fehlberg method based on the shooting technique. Detailed analysis of active quantities of interest has been presented and discussed. The interesting physical quantities (friction factors and Nusselt number) are estimated. Also, the slope of the data point is calculated in order to estimate the amount of decrease/increase in physical quantities.

Keywords Hybrid nanofluid · Nanoparticles · Exponential space-based heat source · Magnetohydrodynamics · Wedge flow

List of symbols

(u, v)	Velocity components in x and y directions ($\mathrm{m\ s^{-1}}$)
T	Temperature of the fluid (K)
T_w	Wall temperature (K)
T_∞	Ambient temperature (K)
B	Variable magnetic field (T)
K	Variable porosity
q_T	Temperature-dependent heat sink/source
q_E	Exponential space-based heat source
n	Dimensionless exponential index (positive)
Ec	Eckert number
Q_T	Temperature-based heat source parameter
Q_E	Exponential space-based heat source parameter
Pr	Prandtl number
C_p	Specific heat $\left(\mathrm{J\,kg^{-1}\,K^{-1}}\right)$
k	Thermal conductivity $\left(\mathrm{W\,m^{-1}\,K^{-1}}\right)$
M	Magnetic parameter
Nu_x	Nusselt number
S_f	Skin friction coefficient
Re_x	Reynolds number
P	Porosity parameter

Greek symbols

θ	Dimensionless temperature
μ	Dynamic viscosity $\left(\mathrm{kg\,m\,s^{-1}}\right)$
ρ	Density $\left(\mathrm{kg\,m^{-3}}\right)$
ν	Kinematic viscosity $\left(\mathrm{m^2\,s^{-1}}\right)$
σ	Electrical conductivity $\left(\mathrm{m^{-1}}\,\Omega^{-1}\right)$
ϕ	The total volume concentration of MoS_2 and Ag
σ	Electrical conductivity $\left(\mathrm{m^{-1}}\,\Omega^{-1}\right)$

Subscripts

l	Base fluid
hnl	Hybrid nanofluid
MoS_2, Ag	Nanoparticles

✉ S. A. Shehzad
sabirali@cuisahiwal.edu.pk

[1] Department of Mathematics, CHRIST (Deemed to be University), Bangalore 560029, India

[2] Department of Mathematics, COMSATS University Islamabad, Sahiwal 57000, Pakistan

[3] School of Mechanical Engineering, Kyungpook National University, Daegu 41566, South Korea

Introduction

The primary investigation related to the enhancement of thermal characteristics due to the suspension of nanoparticles into ordinary liquids was first performed by Choi [1]. The "Nanofluids," the colloidal suspensions of the metallic/non-metallic nanomaterial into the conventional fluids, are proven to exhibit the improved thermophysical properties compared to traditional single-phase coolants. The improved thermal efficiency of these novel fluids is attributed to the nanoparticles' suspension stability, larger effective surface area, Brownian motion, thermophoresis, base fluid micro-convections and the subsequent disruption of the thermoviscous boundary layer. Experimental investigations revealed that heat transfer features and transport characteristics are abundant varieties due to the addition of nanoparticles into ordinary liquids. Nanofluids have numerous applications in nanoscale technology, like solar collectors, air-conditioners, combustors, melt spinning, medicine manufacturing, microelectronics, computer processors and heat exchangers. Further in cancer therapy, wound treatment, hyperthermia and resonance imaging are more supportable for the case of magneto nanofluids (see [2–6]).

The thermophysical abilities of the nanofluids are strongly dependent on the properties of the nanosuspensions and the hosting fluid. Therefore, the desired thermal performance of the nanofluids can be obtained by utilizing the hybrid nanofluids which are prepared by dispersing the dissimilar nanoparticles either in the mixture or in the composite form. Chamkha et al. [7] reported the analysis of transport of hybrid nanofluid flowing between two surfaces. Ghadikolaei et al. [8] utilized the hybrid base fluid and composite nanoparticles to investigate the natural convection in the presence of thermal radiation. Chamkha et al. [9] presented an analysis of transport in a heated horizontal cylinder confined in a square cavity by utilizing single/hybrid nanofluids. Amala and Mahanthesh [10] presented an analytical study to investigate the flow of hybrid nanofluids past a vertical plate in the presence of Hall current and nonlinear Boussinesq approximations. Hayat and Nadeem [11] found that the heat transfer enhancement rate is higher for Ag–Cuo hybrid nanofluid in comparison with mono-nanofluid. Few relevant latest pieces of research on hybrid nanofluids are mentioned in references [12–16]. Another innovative approach to improve the thermal efficiency of the nanofluids is magnetic force-induced convective heat transportation of the magnetic nanofluids. In addition to altering the thermophysical properties of the nanofluids, the implications of external magnetic force offer a driving force for the nanofluid flow [17–19].

The magnetohydrodynamic flow past non-isothermal wedge is of practical importance in relevance to its wide range of applications including magnetohydrodynamic power generation systems, cooling of nuclear reactors, installation of the nuclear accelerators, designing the heat exchangers and measurement techniques of the blood flow. In past, multiple scholars explored the hydrothermal characteristics of magnetohydrodynamic (MHD) flow of electrically conducting conventional fluids over isothermal or non-isothermal wedges (see [20–22] and the references therein). A limited number of numerical and theoretical investigations presented the heat transportation and friction factor aspects of nanofluid flows over a wedge. Khan et al. [23] analysed the Falkner–Skan wedge flow of multiple nanofluids. Their results displayed a strong dependence of heat transfer and friction factor of nanofluids on the nanoparticle concentration, wedge, viscosity and convection parameters. Kandasamy et al. [24] presented a theoretical study on the Hiemenz flow of Cu nanofluid past a permeable wedge by taking into consideration the impact of incident radiation. This study showed a strong influence of thermal satisfaction, buoyancy force, convective radiation, magnetic strength and wedge sheet permeability. Khan and Pop [25] addressed a numerical investigation on the nanofluid flow across a moving wedge by considering the various parameters including nanoparticle pressure gradient, Brownian motion, Lewis number, thermophoresis and wedge moving parameter. The MHD Falkner–Skan flow of aqueous-based nanofluids was studied by Khan et al. [26]. Rashad [27] probed the impact of radiation on the mixed MHD convection of the ferrofluid over a non-isothermal wedge. This study demonstrated that the local Nusselt number has inverse dependence on the thermal radiation, slip factor and wedge surface temperature. The aspects of nanoparticles and Brownian movement in mixed convected nanofluid are reported by Imran et al. [28]. They addressed that the influence of nanoparticles' Brownian diffusion and thermophoresis is more significant on the temperature profiles compared to the nanoparticle volume fraction. The impact of the magnetic parameter is relatively less significant for the nanoparticle concentration and temperature.

The literature survey demonstrates that there exist no studies which focus on the fluid flow and thermal characteristics of hybrid nanofluids over an isothermal wedge. Therefore, the prime objective of the current study is to probe laminar transport of Newtonian composite nanomaterial ($C_2H_6O_2$–H_2O hybrid base liquid + MoS_2–Ag hybrid nanoparticles) in the presence of exponential space and temperature-dependent heat source through the isothermal wedge. Single-phase nanofluid model and boundary layer approximations are implemented to simulate flow and heat transport phenomena of nanofluid. The current work also illustrates the influence of Joule and viscous heating on the

Table 1 Thermophysical properties of hybrid nanofluids [8]

Property	Expression
Dynamic viscosity	$\mu_{\mathrm{hnl}} = \frac{\mu_{\mathrm{f}}}{\left(1-(\phi_{\mathrm{MoS_2}}+\phi_{\mathrm{Ag}})\right)^{2.5}}, \phi = \phi_{\mathrm{MoS_2}} + \phi_{\mathrm{Ag}},$
Density	$\rho_{\mathrm{hnl}} = (1-\phi)\rho_{\mathrm{l}} + \phi_{\mathrm{MoS_2}}\rho_{\mathrm{MoS_2}} + \phi_{\mathrm{Ag}}\rho_{\mathrm{Ag}}$
Heat capacity	$\left(\rho C_{\mathrm{p}}\right)_{\mathrm{hnl}} = (1-\phi)(\rho C_{\mathrm{p}})_{\mathrm{l}} + \phi_{\mathrm{MoS_2}}(\rho C_{\mathrm{p}})_{\mathrm{MoS_2}} + \phi_{\mathrm{Ag}}(\rho C_{\mathrm{p}})_{\mathrm{Ag}}$
Thermal conductivity	$\frac{k_{\mathrm{hnl}}}{k_{\mathrm{l}}} = \left[\frac{\frac{\phi_{\mathrm{MoS_2}}K_{\mathrm{MoS_2}}+\phi_{\mathrm{Ag}}K_{\mathrm{Ag}}}{\phi}+2k_{\mathrm{l}}+2\left(\phi_{\mathrm{MoS_2}}K_{\mathrm{MoS_2}}+\phi_{\mathrm{Cu}}K_{\mathrm{Ag}}\right)-2\phi k_{\mathrm{l}}}{\frac{\phi_{\mathrm{MoS_2}}K_{\mathrm{MoS_2}}+\phi_{\mathrm{Ag}}K_{\mathrm{Ag}}}{\phi}+2k_{\mathrm{l}}-\left(\phi_{\mathrm{MoS_2}}K_{\mathrm{MoS_2}}+\phi_{\mathrm{Ag}}K_{\mathrm{Ag}}\right)+\phi k_{\mathrm{l}}}\right]$
Electrical conductivity	$\frac{\sigma_{\mathrm{hnl}}}{\sigma_{\mathrm{l}}} = 1 + \frac{3\phi\left(\phi_{\mathrm{MoS_2}}\sigma_{\mathrm{MoS_2}}+\phi_{\mathrm{Ag}}\sigma_{\mathrm{Ag}}-\sigma_{\mathrm{l}}\phi\right)}{(\phi_{\mathrm{MoS_2}}\sigma_{\mathrm{MoS_2}}+\phi_{\mathrm{Ag}}\sigma_{\mathrm{Ag}}+2\sigma_{\mathrm{l}}\phi)-\phi\left((\phi_{\mathrm{MoS_2}}\sigma_{\mathrm{MoS_2}}+\phi_{\mathrm{Ag}}\sigma_{\mathrm{Ag}}\right)-\sigma_{\mathrm{l}}\phi)}$

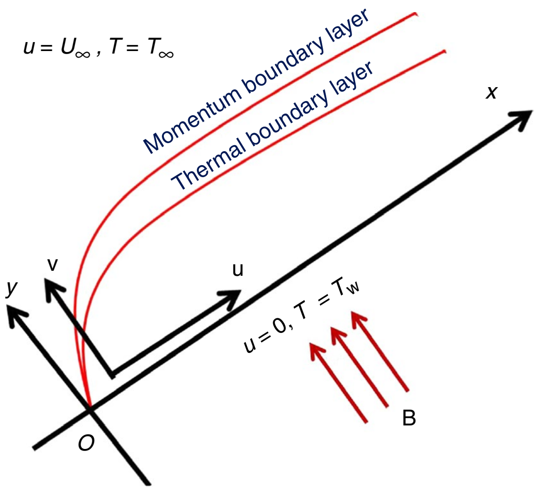

Fig. 1 Schematic diagram of the problem

thermal and viscous characteristics of the hybrid magnetic nanofluids (Table 1).

Formulation of the problem

The non-transient dynamics of Newtonian hybrid nanoliquid ($C_2H_6O_2$–H_2O base liquid + MoS_2–Ag nanoparticles) over an isothermal wedge is considered. The hybrid nanoliquid conducts electricity and incompressible in nature. The motion is due to wedge with an angle $\pi/2$ to ease the computations. The rectangular coordinate system is adapted such that the x axis is along with the wedge and y-axis normal to it (Fig. 1). The variable magnetic dipole and porosity are considered in the analysis. Hybrid base fluid $C_2H_6O_2$–H_2O and hybrid nanoparticles (MoS_2–Ag) are in the thermal equilibrium state, and also there is no slippery between them. The thermophysical values of hybrid base fluid $C_2H_6O_2$–H_2O and nanoparticles (MoS_2 and Ag) are given in Table 2. Through the boundary layer and Boussinesq approximations along with the above-said assumptions, the governing equations can be written as follows:

Continuity equation

$$\frac{\partial u}{\partial x} + \frac{\partial v}{\partial y} = 0. \tag{1}$$

Table 2 Thermophysical properties of $C_2H_6O_2$–H_2O, MoS_2 and Ag (see [8])

Physical properties	Density/ρ	Specific heat/c_p	Thermal conductivity/k	Electrical conductivity/σ	Prandtl number/Pr
Ag	10,490	235	429	6.30×10^{7}	–
MoS_2	5060	397.21	904.4	2.09×10^{4}	–
$C_2H_6O_2$–H_2O	1063.8	3630	0.387	9.75×10^{-4}	25.33

Conservation of linear momentum

$$u\frac{\partial u}{\partial x}+v\frac{\partial u}{\partial y}=U_\infty\frac{\mathrm{d}U_\infty}{\mathrm{d}x}+\frac{\mu_{\mathrm{hnl}}}{\rho_{\mathrm{hnl}}}\frac{\partial^2 u}{\partial y^2}-\left(\frac{\sigma_{\mathrm{hnl}}}{\rho_{\mathrm{hnl}}}B^2+\frac{\mu_{\mathrm{hnl}}}{\rho_{\mathrm{hnl}}}\frac{1}{K}\right)\left(u-U_\infty\right). \quad (2)$$

Conservation of energy

$$u\frac{\partial T}{\partial x}+v\frac{\partial T}{\partial y}=\frac{k_{\mathrm{hnl}}}{\left(\rho C_{\mathrm{p}}\right)_{\mathrm{hnl}}}\frac{\partial^2 T}{\partial y^2}+\frac{\sigma_{\mathrm{hnl}}}{\left(\rho C_{\mathrm{p}}\right)_{\mathrm{hnl}}}B^2u^2+\frac{\mu_{\mathrm{hnl}}}{\left(\rho C_{\mathrm{p}}\right)_{\mathrm{hnl}}}\left(\frac{\partial u}{\partial y}\right)^2+\frac{q_{\mathrm{T}}^*}{\left(\rho C_{\mathrm{p}}\right)_{\mathrm{hnl}}}\left(T-T_\infty\right)+q_{\mathrm{E}}^*\left(T_{\mathrm{w}}-T_\infty\right)\exp\left(-n\sqrt{\frac{2c}{3\nu_{\mathrm{l}}}}yx^{-\frac{1}{3}}\right). \quad (3)$$

The respective boundary conditions are:

$$u=v=0,\quad T=T_{\mathrm{w}},\quad y=0,$$
$$u=U_\infty(x)=cx^{1/3},\quad T\to T_\infty,\quad y\to\infty, \quad (4)$$

where $q_{\mathrm{T}}^*=q_{\mathrm{T}}x^{m-1}$, $q_{\mathrm{E}}^*=q_{\mathrm{E}}x^{\mathrm{m}-1}$ $B=B_0x^{(\mathrm{m}-1)/2}$ and $K=K_0x^{(1-\mathrm{m})}$.

The single-phase nanofluid model assumes that the fluid phase and particles are in thermal equilibrium and move with the same velocity. The effective nanofluid properties are accounted in this model. The effective nanofluid properties are estimated by using convectional mixture theory and phenomenological laws. Specifically, effective thermal conductivity and dynamic viscosity are determined by using modified Brinkman–Garnet and modified Maxwell models correspondingly. The thermophysical properties of hybrid nanofluid are given in Table 1.

Here, u,v are the velocity components in x and y directions, $T, T_{\mathrm{w}}, T_\infty$ the temperature of the fluid, wall temperature and ambient temperature, respectively, B the variable magnetic field, μ the dynamic viscosity, C_{p} the specific heat, K the variable porosity, q_{T} the temperature-dependent heat sink/ source, q_{E} the exponential space-based heat source, n the dimensionless exponential index (positive), c the constant, ρ the density, k the thermal conductivity, $\phi_{\mathrm{MoS_2}}$ and ϕ_{Ag} the volume fractions of MoS_2 and Ag nanoparticles, respectively, ϕ the total volume fraction, ρC_{p} the heat capacity, ν the kinematic viscosity, and the subscripts *hnl* and *l* the corresponding properties of hybrid nanoliquid and base liquid, respectively.

The continuity formula can be satisfied by employing the stream function $\psi(x,y)$ s.t.

$$u=\frac{\partial\psi}{\partial y},\quad v=-\frac{\partial\psi}{\partial x}. \quad (5)$$

We considered the following variables

$$\eta=y\sqrt{\frac{2c}{3\gamma}}x^{-1/3},\quad \psi(x,y)=\sqrt{\frac{3c\gamma}{2}}x^{2/3}f(\eta),\quad \theta(\eta)=\frac{T-T_\infty}{T_{\mathrm{w}}-T_\infty}, \quad (6)$$

The implication of these variables leads to the following expressions:

$$\frac{\mathrm{d}^3f}{\mathrm{d}\eta^3}+\frac{A_2}{A_1}f(\eta)\frac{\mathrm{d}^2f}{\mathrm{d}\eta^2}-\frac{A_2}{2A_1}\left(\frac{\mathrm{d}f}{\mathrm{d}\eta}\right)^2+\left(\frac{A_3}{A_1}M+\frac{1}{P}\right)\left(1-\frac{\mathrm{d}f}{\mathrm{d}\eta}\right)=0, \quad (7)$$

$$\frac{A_4}{\mathrm{Pr}}\frac{\mathrm{d}^2\theta}{\mathrm{d}\eta^2}+A_5f(\eta)\frac{\mathrm{d}\theta}{\mathrm{d}\eta}+A_1\mathrm{Ec}\left(\frac{\mathrm{d}^2f}{\mathrm{d}\eta^2}\right)^2+A_3\mathrm{Ec}M\left(\frac{\mathrm{d}f}{\mathrm{d}\eta}\right)^2+Q_{\mathrm{T}}\theta(\eta)+Q_{\mathrm{E}}\exp(-n\eta)=0, \quad (8)$$

with

$$f(0)=f'(0)=0,\quad \theta(0)=1$$
$$f'(\infty)=1,\quad \theta(\infty)=0.$$

where

$$A_1=\frac{1}{\left(1-(\phi_{\mathrm{MoS_2}}+\phi_{\mathrm{Ag}})\right)^{2.5}},$$

$$A_2=(1-\phi)+\frac{\phi_{\mathrm{MoS_2}}\rho_{\mathrm{MoS_2}}+\phi_{\mathrm{Ag}}\rho_{\mathrm{Ag}}}{\rho_{\mathrm{l}}},$$

$$A_3=1+\frac{3\phi\left(\phi_{\mathrm{MoS_2}}\sigma_{\mathrm{MoS_2}}+\phi_{\mathrm{Ag}}\sigma_{\mathrm{Ag}}-\sigma_{\mathrm{l}}\phi\right)}{(\phi_{\mathrm{MoS_2}}\sigma_{\mathrm{MoS_2}}+\phi_{\mathrm{Ag}}\sigma_{\mathrm{Ag}}+2\sigma_{\mathrm{l}}\phi)-\phi\left((\phi_{\mathrm{MoS_2}}\sigma_{\mathrm{MoS_2}}+\phi_{\mathrm{Ag}}\sigma_{\mathrm{Ag}})-\sigma_{\mathrm{l}}\phi\right)},$$

$$A_4=\left[\frac{\frac{\phi_{\mathrm{MoS_2}}k_{\mathrm{MoS_2}}+\phi_{\mathrm{Ag}}k_{\mathrm{Ag}}}{\phi}+2k_{\mathrm{l}}+2\left(\phi_{\mathrm{MoS_2}}k_{\mathrm{MoS_2}}+\phi_{\mathrm{Ag}}k_{\mathrm{Ag}}\right)-2\phi k_{\mathrm{l}}}{\frac{\phi_{\mathrm{MoS_2}}k_{\mathrm{MoS_2}}+\phi_{\mathrm{Ag}}k_{\mathrm{Ag}}}{\phi}+2k_{\mathrm{l}}-\left(\phi_{\mathrm{MoS_2}}k_{\mathrm{MoS_2}}+\phi_{\mathrm{Ag}}k_{\mathrm{Ag}}\right)+\phi k_{\mathrm{l}}}\right],$$

$$A_5=(1-\phi)+\frac{\left(\phi_{\mathrm{MoS_2}}(\rho C_{\mathrm{p}})_{\mathrm{MoS_2}}+\phi_{\mathrm{Ag}}(\rho C_{\mathrm{p}})_{\mathrm{Ag}}\right)}{(\rho C_{\mathrm{p}})_{\mathrm{l}}},$$

$\mathrm{Ec}=\frac{U_w^2}{C_{\mathrm{p_l}}(T_{\mathrm{w}}-T_\infty)}$ is the Eckert number, $Q_{\mathrm{T}}=\frac{q_{\mathrm{T}}}{c(\rho C_{\mathrm{p}})_{\mathrm{l}}}$ the temperature-based heat source parameter, $Q_{\mathrm{E}}=\frac{q_{\mathrm{E}}}{c(\rho C_{\mathrm{p}})_{\mathrm{l}}}$ the exponential space-based heat source parameter, $\mathrm{Pr}=\frac{\mu_{\mathrm{l}}C_{\mathrm{p_l}}}{k_{\mathrm{l}}}$ the Prandtl number, and $M=\frac{\sigma_{\mathrm{l}}B_0^2}{\rho_{\mathrm{l}}c}$ the magnetic parameter.

Mathematically, expressions of skin friction coefficient and Nusselt numbers in the dimensional form are:

$$S_{\mathrm{f}}=\frac{2\tau_{\mathrm{w}}}{\rho_{\mathrm{l}}U_\infty},\quad \mathrm{Nu_x}=\frac{xq_{\mathrm{w}}}{k_{\mathrm{l}}\left(T_{\mathrm{w}}-T_\infty\right)},$$

where $\tau_w = \mu_{hnl}\frac{\partial u}{\partial y}$ and $q_w = -k_{hnl}\frac{\partial T}{\partial y}$.

The dimensionless form of the above expressions is

$$\sqrt{Re_x}S_f = \sqrt{\frac{8}{3}}A_1 f''(0),$$

$$\frac{Nu_x}{\sqrt{Re_x}} = -\sqrt{\frac{8}{3}}A_4\theta'(0),$$

where $Re_x = \frac{U_\infty x}{\nu_l}$ is the Reynolds number.

Results and discussion

Here, our emphasis is to scrutinize the features of exponential space- and thermal-based heat source for composite nanomaterial's nanofluid flow over an isothermal wedge by considering the aspects of viscous and Joule heating. In order to solve the governing system of equations, we made the numerical computations by Runge–Kutta–Fehlberg-based shooting scheme. Validation and detailed procedure of the method can be found in [18, 19].

Firstly, the skin friction coefficient is analysed by varying magnetic and porosity parameters. In the numeric

Table 3 Variation in skin friction for different values when $Ec = 1.5$, $M = 2$, $Pr = 25.34$, $Q_T = Q_E = 0.02$, $n = 0.5$, $P = 1.5$

M	P	S_f		
		$\phi_{MoS_2} = \phi_{Ag} = 0.02$	$\phi_{MoS_2} = 0.02$ $\phi_{Ag} = 0$	$\phi_{MoS_2} = 0$ $\phi_{Ag} = 0.02$
1		2.252276	2.075331	2.136126
2		2.890492	2.647766	2.739438
3		3.414822	3.120615	3.235256
Slope		0.581273	0.522642	0.549565
	0.1	6.232125	5.873613	5.916415
	0.5	3.563174	3.30477	3.379504
	0.9	3.130468	2.882989	2.967842
Slope		−3.87707125	−3.73828	−3.68571625

Table 4 Variation in Nusselt number for different values when $Ec = 1.5$, $M = 2$, $Pr = 25.34$, $Q_T = Q_E = 0.02$, $n = 0.5$, $P = 1.5$

M	P	Ec	Q_T	Q_E	Nu_x		
					$\phi_{MoS_2} = \phi_{Ag} = 0.02$	$\phi_{MoS_2} = 0.02$ $\phi_{Ag} = 0$	$\phi_{MoS_2} = 0$ $\phi_{Ag} = 0.02$
1					−34.8594	−30.4202	−32.2758
2					−62.5768	−53.935	−57.7475
3					−91.5485	−78.5204	−84.336
Slope					−28.34455	−24.0501	−26.0301
	0.1				−129.98	−117.524	−120.993
	0.5				−76.4017	−67.025	−70.6892
	0.9				−67.5213	−58.6228	−62.3745
Slope					78.073375	73.6265	73.273125
		0.5			−18.9067	−16.1493	−17.3678
		1			−40.7418	−35.0421	−37.5576
		1.5			−62.5768	−53.935	−57.7475
Slope					−43.6701	−37.7857	−40.3797
			0		−59.8401	−51.4746	−55.1946
			0.1		−64.0402	−66.0351	−70.2094
			0.2		−65.8693	−88.6149	−93.0936
Slope					−30.146	−185.7015	−189.495
				0.1	−75.9187	−55.3938	−59.1832
				0.2	−100.345	−57.2172	−60.9779
				0.3	−139.556	−59.0407	−62.7726
Slope					−318.1865	−18.2345	−17.947

computations, the default values of effective parameters are set as Ec = 1.5, $M = 2$, Pr = 25.34, $Q_T = Q_E = 0.02$, $n = 0.5$ and $P = 1.5$ unless otherwise mentioned. The Newtonian hybrid nanoliquid is considered, and the results are presented for three different nanofluids: hybrid nanofluid ($\phi_{MoS_2} = \phi_{Ag} = 0.02$), MoS_2 nanofluid and Cu nanofluid. Table 3 demonstrates the impact of magnetic and porosity parameters on the skin friction coefficient. By increasing the magnetic parameter, an increase in skin friction for all three cases of volume fractions (fluids) is observed. The average slopes of S_f and M for three volume fraction cases are also calculated. The impact of increased porosity parameter results in a decrease in S_f for volume fraction cases under consideration. It is also scrutinized from Table 3 that S_f has a reverse trend for increased M and P. Moreover, the average slopes of S_f and M are positive, while the slopes of S_f and P are negative. Table 4 shows the Nusselt number trend by varying M, P, Ec, Q_T and Q_E. Here, also the same three cases of volume fractions are mentioned in Table 3. Heat transfer rate increases due to enhancement in magnetic parameter, Eckert number, temperature-based heat source parameter and exponential space-based heat source parameter. The rate of heat transfer declines for increased porosity parameter. The slopes of Nu_x and P for three volume fraction cases are positive, whereas all other slopes are negative as mentioned in Table 4.

Now, we discuss the graphical results of physical parameters on velocity and temperature fields. Figure 2a, b shows

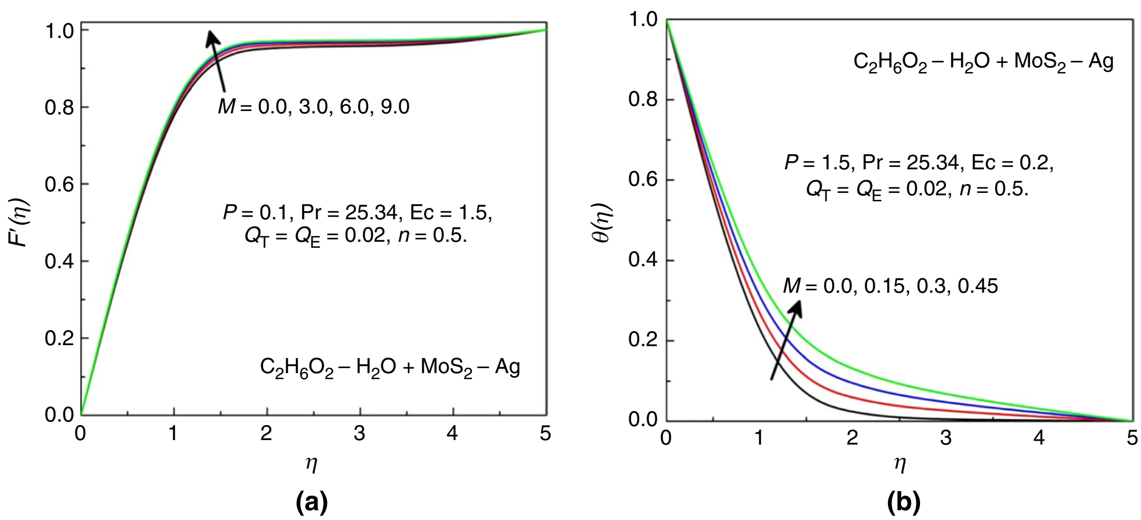

Fig. 2 Behavior of hybrid nanofluid **a** velocity and **b** temperature for various M

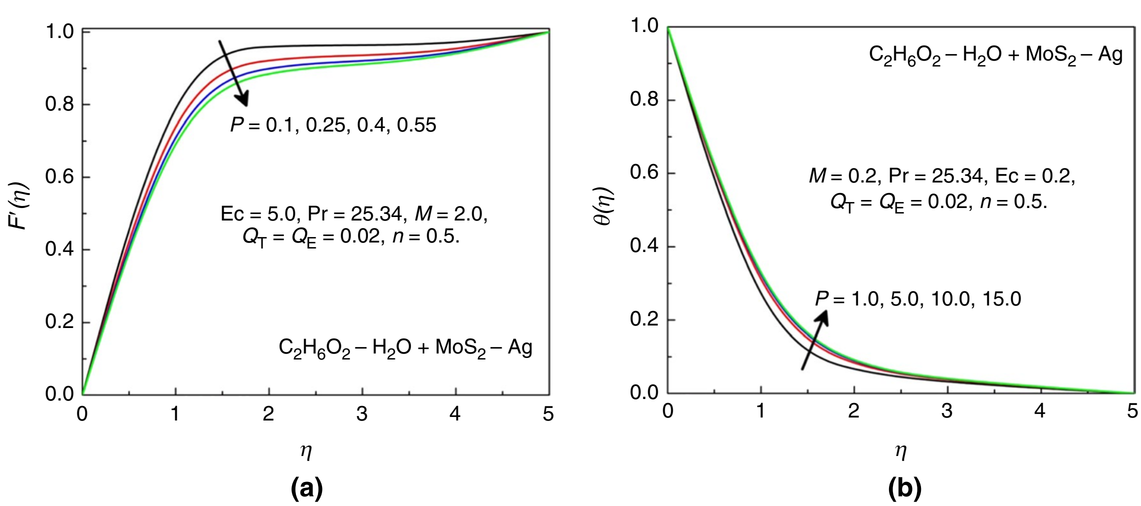

Fig. 3 Behavior of hybrid nanofluid **a** velocity and **b** temperature for various P

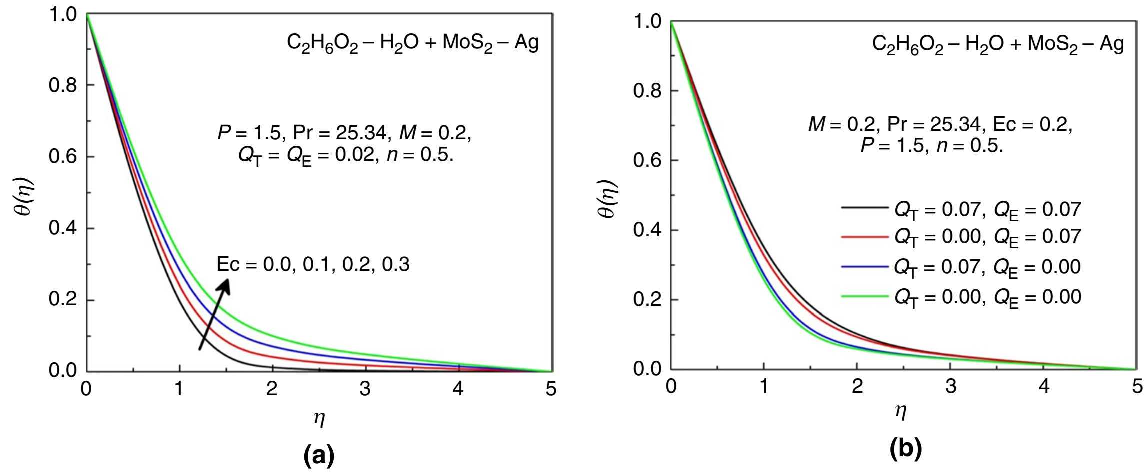

Fig. 4 Behavior of hybrid nanofluid temperature for various **a** Ec and **b** Q_T

the behaviour of hybrid nanofluid velocity $f'(\eta)$ and temperature $\theta(\eta)$ for various values of M. As apparent from Fig. 2a, the velocity profiles have increasing nature for the larger magnetic parameter. The temperature distribution exhibits an increasing trend for higher values of the magnetic field parameter. Thermal boundary layer also increased. Physically, when magnetic parameter number increases, then Lorentz force produces more frictional forces between fluid particles due to which temperature and its respective boundary layer thickness elevate. In Fig. 2a, b, the first case $M = 0$ describes the hydrodynamic fluid flow case, whereas the nonzero values of M predict the hydromagnetic flow of hybrid nanofluid. Figure 3a, b illustrates the consequences of the porosity parameter of $f'(\eta)$ and $\theta(\eta)$. An increase in porosity parameter produces more resistance to the fluid flow due to porosity of the surface; therefore, the velocity curves have a declining trend for $P = 0.1,\ 0.25,\ 0.4,\ 0.55$ (Fig. 3a). From Fig. 3b, it is noticed that the temperature curves enhanced by selecting $P = 1, 5, 10, 15$. It is also noticed that the results are significant for smaller values of porosity parameter as compared to larger values of P. The Eckert number expresses the relationship between a flow's kinetic energy and the boundary layer enthalpy difference and is used to characterize heat transfer dissipation. The Eckert number effect on Newtonian hybrid nanoliquid temperature field is elaborated in Fig. 4a. Similar to the impact of magnetic and porosity parameters, the temperature curves also enhance for increasing Eckert number. Due to frictional heating, heat produced in the fluid which caused an enhancement in temperature field as well as the thickness of the thermal boundary layer. The case $\mathrm{Ec} = 0$ depicts that the effect of viscous and Joule heating is neglected. The combined influence of temperature and exponential space-based heat source parameters on temperature field is illustrated in

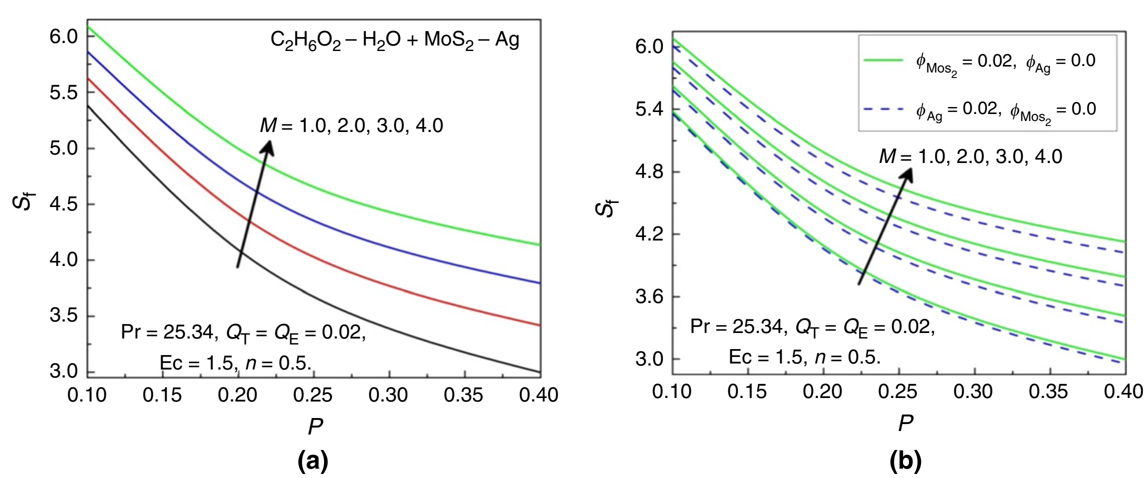

Fig. 5 Behavior of hybrid nanofluid skin friction coefficient for various **a** P and **b** M

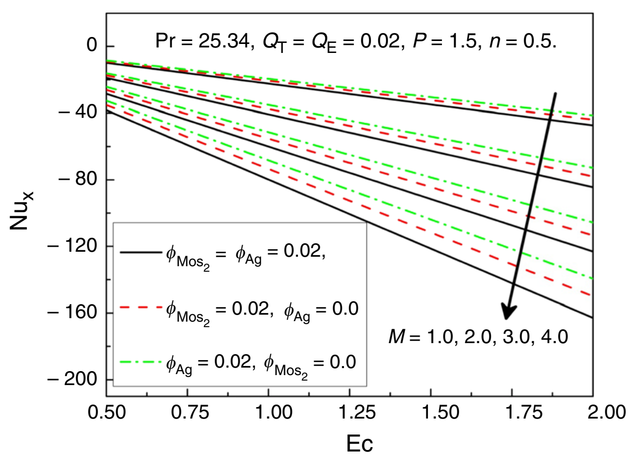

Fig. 6 Behavior of hybrid nanofluid Nusselt number for various Ec and M

Fig. 4b. Here, four different cases of Q_T and Q_E are considered. It is very clear that the presence of thermal-based heat source and exponential space-based heat source augments the thermal boundary layer thickness. This is due to the fact that a heat source aspect introduces additional heat in the fluid system due to which the temperature of hybrid nanofluid is enhanced. It is also depicts that impact of exponential space-based heat source aspect is more prominent than that of temperature-based heat source aspect.

Figure 5a shows the variations of skin friction coefficient versus porosity parameter and magnetic parameter. Figure 5a depicts that the skin friction increases for larger magnetic parameter values and decreases for larger porosity parameter. Figure 5b describes the outcomes of S_f against P by varying M. The two cases of volume fractions $\varphi_{MoS_2} = 0.02, \quad \varphi_{Ag} = 0$ and $\varphi_{MoS_2} = 0, \varphi_{Ag} = 0.02$ are considered to mention the influence of skin friction coefficient. It is perceived that S_f preserves an increasing tendency. Moreover, the values of S_f are larger for volume fraction $\varphi_{MoS_2} = 0.02, \varphi_{Ag} = 0$ than in the case of $\varphi_{MoS_2} = 0, \varphi_{Ag} = 0.02$. Nusselt number versus Eckert number effect for four different values of the magnetic parameter is shown in Fig. 6. Here, we opt four different cases of volume fractions $\varphi_{MoS_2} = \varphi_{Ag} = 0.02$, $\varphi_{MoS_2} = 0.02$, $\varphi_{Ag} = 0$ and $\varphi_{MoS_2} = 0$, $\varphi_{Ag} = 0.02$. Figure 6 describes the variation in Nusselt number against Eckert number showing decreasing behaviour by fixing the magnetic parameter.

Conclusions

The following key features are extracted from this analysis:

- The temperature profile and its relevant boundary layer thickness have increasing nature for the larger magnetic parameter.
- The exponential heat source aspect is better suited for applications involved high heating processes.
- Both exponential space-based heat source and thermal-based heat source aspects are favourable for hybrid nanofluid temperature profiles.
- The thermal boundary layer thickness is higher for hybrid nanofluid in comparison with the mono-nanofluids.
- An increase in porosity parameter generates much resistance to liquid flow due to which the velocity curves show declining tendency.
- The frictional heating generates more heat in the fluid that results in improving the temperature field. Thus, the Eckert number is useful in determining the relative importance in a heat transfer situation of the kinetic energy of a flow.
- The skin friction increases for a stronger magnetic field.
- The variation in Nusselt number against Eckert number shows decreasing behaviour by fixing the magnetic parameter.

Acknowledgements The first author (B. Mahanthesh) gratefully acknowledges the support of the Management of CHRIST (Deemed to be University), Bangalore, India, for pursuing this work. Also, we are very grateful for the editor and reviewers for their constructive suggestions.

Funding There are no funders to report for this submission.

Compliance with ethical standards

Conflict of interest The authors declare that they have no conflict of interest.

References

1. Choi SUS. Enhancing thermal conductivity of fluids with nanoparticles. In: ASME, FED 231/MD; 1995. p. 99–105.
2. Milanese M, Iacobazzi F, Colangelo G, de Risi A. An investigation of layering phenomenon at the liquid–solid interface in Cu and CuO based nanofluids. Int J Heat Mass Trans. 2016;103:564–71.
3. Visconti P, Primiceri P, Costantini P, Colangelo G, Cavalera G. Measurement and control system for thermosolar plant and performance comparison between traditional and nanofluid solar thermal collectors. Int J Smart Sens Intell Syst 2016; 9(3).
4. Colangelo G, Milanese M. Numerical simulation of thermal efficiency of an innovative Al_2O_3 nanofluid solar thermal collector: influence of nanoparticles concentration. Therm Sci. 2017;21:2769–79.
5. Colangelo G, Favale E, Miglietta P, Milanese M, de Risi A. Thermal conductivity, viscosity and stability of Al_2O_3-diathermic oil nanofluids for solar energy systems. Energy. 2016;95:124–36.
6. Ambreen T, Kim MH. Heat transfer and pressure drop correlations of nanofluids: a state of art review. Renew Sustain Energ Rev. 2018;91:564–83.
7. Chamkha AJ, Dogonchi AS, Ganji DD. Magneto-hydrodynamic flow and heat transfer of a hybrid nanofluid in a rotating system

among two surfaces in the presence of thermal radiation and Joule heating. AIP Adv. 2019;9(2):025103.
8. Ghadikolaei SS, Gholinia M, Hoseini ME, Ganji DD. Natural convection MHD flow due to MoS_2–Ag nanoparticles suspended in $C_2H_6O_2H_2O$ hybrid base fluid with thermal radiation. J Taiwan Inst Chem Eng. 2019;97:12–23.
9. Chamkha AJ, Doostanidezfuli A, Izadpanahi E, Ghalambaz MJ. Phase-change heat transfer of single/hybrid nanoparticles-enhanced phase-change materials over a heated horizontal cylinder confined in a square cavity. Adv Powder Technol. 2017;28(2):385–97.
10. Amala S, Mahanthesh B. Hybrid nanofluid flow over a vertical rotating plate in the presence of hall current, nonlinear convection and heat absorption. J Nanofluids. 2018;7(6):1138–48.
11. Hayat T, Nadeem S. Heat transfer enhancement with Ag–CuO/water hybrid nanofluid. Results Phys. 2017;7:2317–24.
12. Shruthy M, Mahanthesh B. Rayleigh-Bénard convection in Casson and hybrid nanofluids: an analytical investigation. J Nanofluids. 2019;8(1):222–9.
13. Ashlin TS, Mahanthesh B. Exact solution of non-coaxial rotating and non-linear convective flow of Cu–Al_2O_3–H_2O hybrid nanofluids over an infinite vertical plate subjected to heat source and radiative heat. J Nanofluids. 2019;8(4):781–94.
14. Mehryan SA, Izadi M, Namazian Z, Chamkha AJ. Natural convection of multi-walled carbon nanotubes-Fe_3O_4/water magnetic hybrid nanofluid flowing in porous medium considering the impacts of magnetic field-dependent viscosity. J Therm Anal Calorim. 2019;138(2):1541–55.
15. Mohebbi R, Izadi M, Delouei AA, Sajjadi H. Effect of MWCNT–Fe_3O_4/water hybrid nanofluid on the thermal performance of ribbed channel with apart sections of heating and cooling. J Therm Anal Calorim. 2019;135(6):3029–42.
16. Maskeen MM, Zeeshan A, Mehmood OU, Hassan M. Heat transfer enhancement in hydromagnetic alumina–copper/water hybrid nanofluid flow over a stretching cylinder. J Therm Anal Calorim. 2019;138(2):1127–36.
17. Nkurikiyimfura I, Wang Y, Pan Z. Heat transfer enhancement by magnetic nanofluids—a review. Renew Sustain Energy Rev. 2013;21:548–61.
18. Mahanthesh B, Gireesha BJ, Shashikumar NS, Shehzad SA. Marangoni convective MHD flow of SWCNT and MWCNT nanoliquids due to a disk with solar radiation and irregular heat source. Phys E Low Dimens Syst Nanostruct. 2017;94:25–30.
19. Mahanthesh B, Gireesha BJ, Shehzad SA, Rauf A, Kumar PS. Nonlinear radiated MHD flow of nanoliquids due to a rotating disk with irregular heat source and heat flux condition. Phys B Condens Matter. 2018;537:98–104.
20. Chamkha AJ, Mujtaba M, Quadri A, Issa C. Thermal radiation effects on MHD forced convection flow adjacent to a non-isothermal wedge in the presence of a heat source or sink. Heat Mass Transf. 2003;39(4):305–12.
21. Rashidi MM, Ali M, Freidoonimehr N, Rostami B, Hossain MA. Mixed convective heat transfer for MHD viscoelastic fluid flow over a porous wedge with thermal radiation. Adv Mech Eng. 2014;6:735939.
22. Ishak A, Nazar R, Pop I. MHD boundary-layer flow of a micropolar fluid past a wedge with constant wall heat flux. Commun Nonlinear Sci Numer Simul. 2009;14(1):109–18.
23. Khan WA, Hamad MA, Ferdows M. Heat transfer analysis for Falkner-Skan boundary layer nanofluid flow past a wedge with convective boundary condition considering temperature-dependent viscosity. Proc Inst Mech Eng Part N J Nanoeng Nanosyst. 2013;227(1):19–27.
24. Kandasamy R, Muhaimin I, Khamis AB, BinRoslan R. Unsteady Hiemenz flow of Cu-nanofluid over a porous wedge in the presence of thermal stratification due to solar energy radiation: Lie group transformation. Int J Therm Sci. 2013;65:196–205.
25. Khan WA, Pop I. Boundary layer flow past a wedge moving in a nanofluid. Math Probl Eng. 2013;2013:1–7.
26. Khan U, Ahmed N, Mohyud-Din ST. Heat transfer enhancement in hydromagnetic dissipative flow past a moving wedge suspended by H_2O–aluminum alloy nanoparticles in the presence of thermal radiation. Int J Hydrog Energy. 2017;42(39):24344–634.
27. Rashad AM. Impact of thermal radiation on MHD slip flow of a ferrofluid over a non-isothermal wedge. J Magn Magn Mater. 2017;422:25–31.
28. Ullah I, Shafie S, Khan I, Hsiao KL. Brownian diffusion and thermophoresis mechanisms in Casson fluid over a moving wedge. Results Phys. 2018;9:183–94.